Published in New Phytologist 174, issue 1, 63-76, 2007
which should be used for any reference to this work

In vivo visualization of F-actin structures during the development of the moss *Physcomitrella patens*

Andrija Finka[1], Didier G. Schaefer[2], Younousse Saidi[3], Pierre Goloubinoff[3] and Jean-Pierre Zrÿd[3]

[1]SV/IBI, EPFL, Station 15, CH–1015 Lausanne, Switzerland; [2]Station de Génétique et d'Amélioration des Plantes, INRA, Route de St Cyr, F–78026 Versailles, France; [3]Department of Plant Molecular Biology, University of Lausanne, CH–1015 Lausanne, Switzerland

Author for correspondence: *Jean-Pierre Zrÿd, Tel: +41 21 6924223, Fax: +41 21 6924195, Email: Jean-Pierre.Zryd@unil.ch*

Summary

• The '*in planta*' visualization of F-actin in all cells and in all developmental stages of a plant is a challenging problem. By using the soybean heat inducible *Gmhsp17.3B* promoter instead of a constitutive promoter, we have been able to label all cells in various developmental stages of the moss *Physcomitrella patens*, through a precise temperature tuning of the expression of green fluorescent protein (GFP)-talin.

• A short moderate heat treatment was sufficient to induce proper labeling of the actin cytoskeleton and to allow the visualization of time-dependent organization of F-actin structures without impairment of cell viability.

• In growing moss cells, dense converging arrays of F-actin structures were present at the growing tips of protonema cell, and at the localization of branching. Protonema and leaf cells contained a network of thick actin cables; during de-differentiation of leaf cells into new protonema filaments, the thick bundled actin network disappeared, and a new highly polarized F-actin network formed.

• The controlled expression of GFP-talin through an inducible promoter improves significantly the '*in planta*' imaging of actin.

Key words: actin microfilament, ARP3, cell polarity, cytoskeleton, green fluorescent protein (GFP)-talin, heat-shock promoter, moss, *Physcomitrella patens*.

Introduction

The cytoskeleton is a dynamic framework of structural proteins, which are critical to many cellular processes. The two major constituents of the cytoskeleton networks are the actin microfilaments (or F-actin) and the microtubules. Actin filaments are associated with cell polarity and organelle trafficking, both processes being under the control of internal and environmental stimuli. One experimental approach to describe cellular differentiation and tissue morphogenesis is the careful analysis of the intricate dynamic changes that take place in the cytoskeleton (see reviews by Kost *et al.*, 2002; Smith, 2003; Wasteneys & Galway, 2003).

Mosses are organisms well suited for the study of subcellular actin structures in plants, since the structural organization of actin can be observed in the context of complete cell lineages (Schnepf *et al.*, 1986). In the moss *Physcomitrella patens* (Funariales), the gametophyte development begins with the two-dimensional growth of tip-growing protonemata made of chloronema cells that undergo a developmental transition to caulonema cells (Schaefer, 2001). The photosynthetic chloronema cells contain many large, round chloroplasts and their cell walls are perpendicular to the growth axis of the filament. By contrast, the developing caulonemal cells contain less small elliptical chloroplasts and cell walls have an oblique orientation with respect to the axis of the filament. The formation of gametophores or leafy shoots constitutes a transition to three-dimensional growth, followed by an attachment of the plant to the substrate through rhizoid filaments. Complex organs of both gametophyte and sporophyte, are made of only a few cell

layers, allowing microscopic observations of live cells throughout the whole life cycle of the plant (Schaefer & Zryd, 2001; Schaefer, 2001). Studies of actin cytoskeleton in mosses have been limited to the analysis of rhodamine–phalloidin stained protonemata, whereas in other moss cell types, the description of the actin structures is incomplete. Longitudinally oriented actin cables have been detected in the caulonemal cells of *P. patens* (Doonan *et al.*, 1988) as well as in the protonemata of both *Ceratodon purpureus* (Meske & Hartmann, 1995; Walker & Sack, 1995) and *Funaria hygrometrica* (Quader & Schnepf, 1989). In *Funaria*, during side-branch initiation, particular F-actin arrays are present at the prospective outgrowth sites, which could represent actin organizing centers near the plasma membrane.

In vivo visualization of actin microfilament by noninvasive labeling is a prerequisite for adequate study of the behavior of actin microfilament during cell differentiation. The green fluorescent protein (GFP) fused in-frame to F-actin binding domain of proteins such as talin, plastin or fimbrin has been used with partial success in plant cells (Kost *et al.*, 1998; Kovar *et al.*, 2001; Timmers *et al.*, 2002; Ketelaar *et al.*, 2004; Sheahan *et al.*, 2004). Green fluorescent protein tagged to the F-actin binding domain of mouse talin – GFP-talin (Kost *et al.*, 1998) – or human talin (Takemoto *et al.*, 2003; Kwok & Hanson, 2004) has been used to describe plant actin cytoskeleton in a majority of reports. Yet, constitutive expression of GFP-talin under the 35S promoter was found to be too weak for a clear observation of F-actin in some *Arabidopsis* cells and tissues (El-Assall *et al.*, 2004). By contrast, the expression of GFP-talin under strong Lat52 promoter inhibited growth of tobacco pollen tubes (Kost *et al.*, 1998). The use of the alcohol inducible promoter to activate GFP-talin expression is deleterious to the growth in *Arabidopsis* root hairs and to the actin network organization (Ketelaar *et al.*, 2004).

Using stable transgenic *P. patens* bearing the *uidA* gene or the GFP-talin under the control of the soybean *Gmhsp17.3B* promoter, we have previously shown that the synthesis and the accumulation of the GUS reporter enzyme or of GFP-talin can be tightly controlled (Saidi *et al.*, 2005). Varying the induction temperature or the time of induction under conditions that do not affect the viability or the fitness of the plants allowed the fine-tuning of GFP-talin expression. We compared the efficacy of the 35S CaMV constitutive promoter with that of the conditional inducible promoter *Gmhsp17.3B* for optimal labeling of actin structures with GFP-talin at different developmental stages in *P. patens*. The extent and duration of the labeling could be adjusted quantitatively to allow a precise *in vivo* labeling without hampering moss physiology. By controlling the GFP-talin amounts, we could observe for the first time the fine organization of actin microfilaments during all the developmental stages of the moss gametophyte, giving new insights upon the dynamic changes in the architecture of the plant actin cytoskeleton.

Materials and Methods

Construction of plasmid pHSP-GT-AH108

The pHSP-GT construct was generated by replacing the *Nco*I–*Eco*RI GUS-CaMVter fragment of HSP-GUS plasmid (Saidi *et al.*, 2005) with a *Nco*I–*Eco*RI fragment from pYSC14 (Kost *et al.*, 1998) bearing a GFP-Talin-NOSter cassette. Finally, a 4.7 kb *Kpn*I fragment from pBS-BAMH108 vector (A. Finka, unpublished) containing a hygromycin resistance cassette driven by the rice actin-1 gene promoter (McElroy *et al.*, 1991) and a 1.9 kb of PP-108 genomic locus (Schaefer & Zryd, 1997) was inserted in the *Kpn*I restriction site of pHSP-GT vector to create the pHSP-GT-AH108 targeting vector used in moss transformation.

Plant tissue culture, protoplast transformation and isolation of transgenic lines

Moss strains of *P. patens* B.S.G. was grown axenically on either solid minimal medium (Ashton & Cove, 1977) or solid medium supplemented with 2.7 mM ammonium tartrate (Merck, Harlow, UK) and 25 mM glucose (Fluka, Milwaukee, WI, USA) and under defined light conditions of 16 h of light and 8 h of darkness at 25°C. The light intensity used in this study was 60 μmol m^{-2} s^{-1} for white light. Plants were subcultured every 7 d. Chloronemal cells were obtained on supplemented medium 5–6 d after inoculation. Monitoring of caulonemal cells and gametophore growth was performed on plants maintained on solid minimal medium. Isolation of protoplasts, polyethylene glycol–mediated transformation, regeneration and hygromycin selection were performed as described previously (Schaefer & Zryd, 1997).

The 35S-GT lines were generated by cotransformation of equimolar amounts of pYSC14 (Kost *et al.*, 1998) and pGL108 (Schaefer & Zryd, 1997) that was linearized by *Cla*I, whereas HGT lines were obtained upon transformation by pHSP-GT-AH108. All these expressing vectors were targeted to the PP-108 locus (Schaefer & Zryd, 1997; Saidi *et al.*, 2005). The ARP3 insertional mutant cell line was generated by targeting the locus with the plasmid pGAKO-neo. This plasmid was constructed by insertion of a 3 kb *Eco*RI/*Sac*I portion of the *PpARP3* gene (GenBank Accession No. AM287016) into the *Eco*RI/*Sac*I-digested pGEM-T Easy vector (Promega, Madison, WI, USA) to generate pGEM3.0/*Eco*RI-*Sac*I. The *Ava*I/Eco RV fragment was then deleted and replaced by the kanamycin resistance cassette to generate the plasmid pGAKO-neo.

Heat treatments

The cellophane disks supporting moss tissue were transferred to preheated solid medium plates at 37°C, which were sealed with parafilm and placed into the cabinet at the same

temperature. After treatment, the disks were returned onto the original plates and placed in standard growth conditions at 25°C. The isolated protoplasts were embedded in solid medium, then incubated 24 h in darkness and further regenerated in standard growth conditions. One part of the cellophane disk containing the protoplasts was thermally treated over 6 d, as described earlier. After each inducing treatment, we followed the localization of induced GFP-talin in cells as indicated.

Treatment with cytoskeleton-affecting drugs

The microfilament and microtubule-depolymerizing drugs, cytochalasin B and Latrunculin B were dissolved in ethanol at 4 mM, whereas oryzalin (Calbiochem, La Jolla, CA, USA) was dissolved in water at 100 mM. These stocks were diluted to the required concentration with distilled water. The drug solution was directly applied to the moss protonemata after the heat shock. Observations were made 12–16 h after drug application.

Immunoblotting

Plant tissue (approx. 100 mg) was ground directly in 100 µl of sample buffer (100 mM Tris; pH 6.8, 20 mM ethylenediaminetetraacetic acid (EDTA); pH 6.8, 20% glycerol, 4% sodium dodecyl sulphate (SDS), 20 mM β-mercaptoethanol), incubated for 1 h at 40°C and briefly centrifuged. Proteins were quantified by Lowry assay (Lowry *et al.*, 1951) and 20 µg were loaded on a 12% polyacrylamide gel. Polypeptides were separated by SDS–polyacrylamide gel electrophoresis (SDS-PAGE) and electrotransferred onto a 0.2 µm nitrocellulose membrane (Bio-Rad, Marnes-la-Coquette, France) at 100 V for 1 h in transfer buffer (25 mM Tris, 192 mM glycine and 20% methanol). The membrane was briefly stained in 2% Ponceau S (Sigma, St Louis, MO, USA) to confirm equal loading and protein transfer and then blocked for 1 h in TTBS buffer (20 mM Tris; pH 7.6, 1.37 M NaCl, 0.1% Tween 20) containing 1% nonfat dry milk, and subsequently incubated for 1 h in mouse monoclonal anti-GFP primary antibody (1 : 2000; Roche, Indianapolis, IN, USA). Following three 10-min rinses in TTBS, the membrane was incubated in antimouse horseradish peroxidase-conjugated secondary antibody in TTBS (1 : 2000; Sigma) for approx. 1 h. The membrane was washed and then developed using the chemiluminescent Immunstar kit (BioRad) according to manufacturer's instructions. Upon detection of GFP-talin fusion protein, the blot was stripped (100 mM 2-mercaptoethanol, 2% SDS, 62.5 mM Tris-Cl pH 6.7) at 50°C for 30 min. Following washing and blocking, the blot was probed with the monoclonal antiactin antibody C4 (1 : 1000; ICN Biomedicals Inc., Aurora, OH, USA) overnight at 4°C and developed as already described.

Live cell microscopy and image analysis

For confocal microscopy, carefully excised pieces of cellophane containing undamaged moss tissue were transferred into the LabTek II glass slide chamber (Nalge Nunc International, Rochester, NY, USA) in inverted position and covered by a block of solid agar medium. Confocal microscopy was performed on a TCS SP2 system using an inverted microscope (Leica-DMRE). A krypton–argon laser (488 nm line) was used for excitation. To distinguish between the GFP fluorescence and red autofluorescence of chloroplasts, the bandwidth mirror settings for discriminating between the two signals were 504/531 for GFP and 634/696 for chloroplasts. The two channels were allocated false green (GFP) and red chloroplast colors. The projections of image stacks were processed using PHOTOSHOP 6.0 software (Adobe Systems).

Results

Generation of GFP-talin expressing transgenic lines

In order to visualize *in vivo* the actin cytoskeleton in *P. patens*, we generated transgenic strains expressing the F-actin marker GFP-talin driven either by the 35S CaMV promoter (lines 35S-GT, constitutive expression), or by the heat-inducible soybean *Gmhsp17.3B* promoter (HGT strains, heat-inducible expression). Two 35S-GT strains and 10 HGT lines were obtained that carried between three and six tandem repeats of the reporter construct integrated into the genomic locus PP-108 (data not shown). To determine the kinetic of GFP-talin expression in HGT lines, we submitted 1-wk-old colonies from each of the 10 HGT lines to a 37°C heat shock (HS) of increasing duration and examined the tissue by fluorescence microscopy, 16 h after the heat treatment. Untreated samples showed no labeling and we could not detect presence of GFP-talin by immunoassay (Fig. 1a). By contrast, following a 1-h heat treatment and 16 h recovery at 25°C, all strains, showed a uniform labeling of the actin cytoskeleton in all cells of all samples. Shorter or milder heat treatment induced weaker and uneven labeling patterns (Fig. 1b). Immunoblot analysis also showed that a 1-h HS enabled maximal production of GFP-talin without altering the amount of intracellular globular actin (Fig. 1a). The labeling was very similar in all the strains and two of them (HGT1 and HGT10, four to six plasmid copies per genome) were chosen for further characterization of the actin cytoskeleton. We also followed actin labeling over 72 h following a 1-h HS at 37°C and found that the strongest GFP fluorescence can be observed 12 h and 18 h after HS (Fig. 1c); it then progressively declined and became undetectable after 60–72 h (not shown). The turnover of GFP-talin, with a half life of 6 d, is then much faster than the turnover reported previously for GUS under the same conditions (Saidi *et al.*, 2005) reducing the possible toxic effects of the overexpression of GFP-talin.

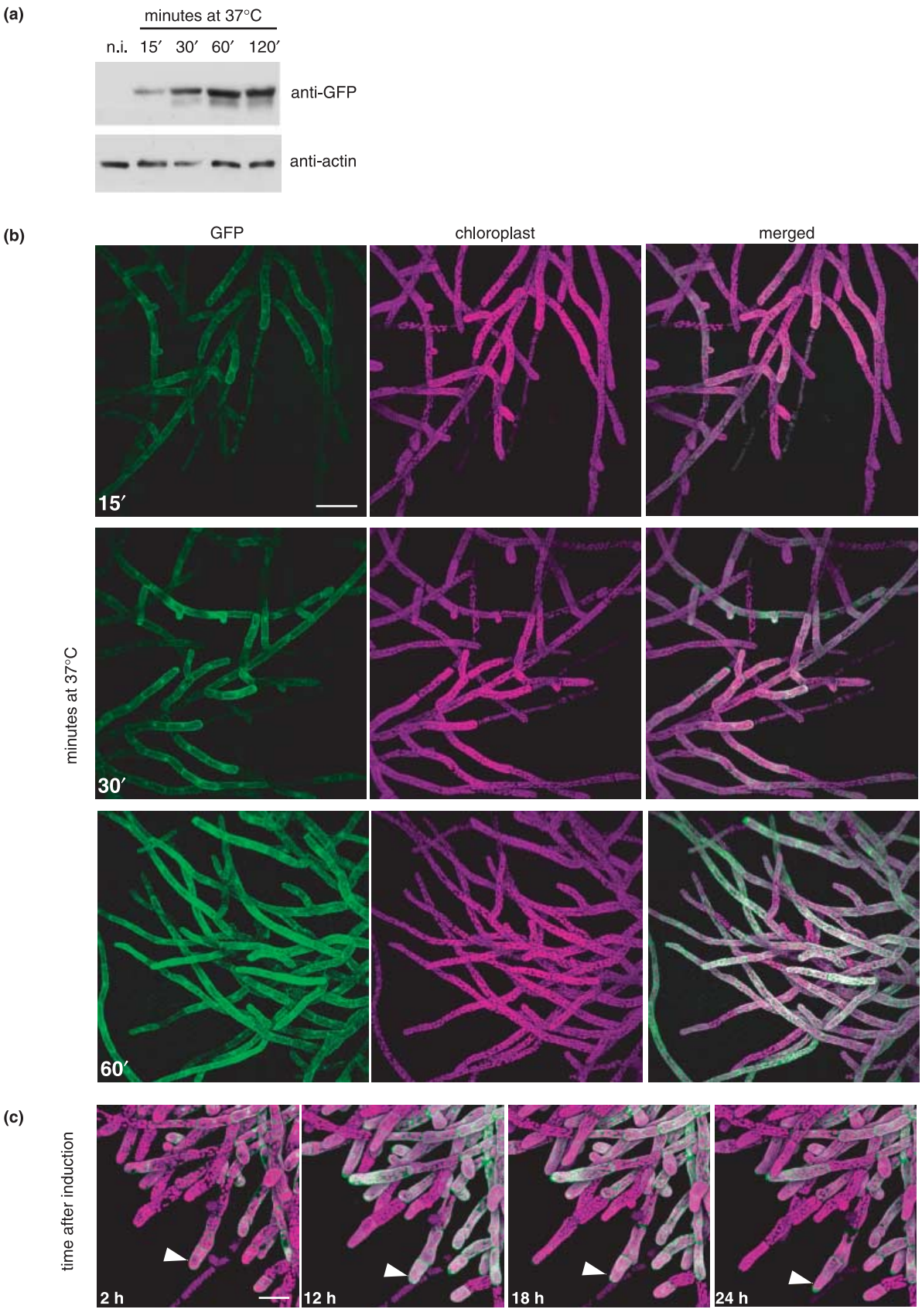
(a)
minutes at 37°C
n.i.
15′
30′
60′
120′
anti-GFP
anti-actin
(b)
GFP
chloroplast
merged
minutes at 37°C
15′
30′
60′
(c)
time after induction
2 h
12 h
18 h
24 h

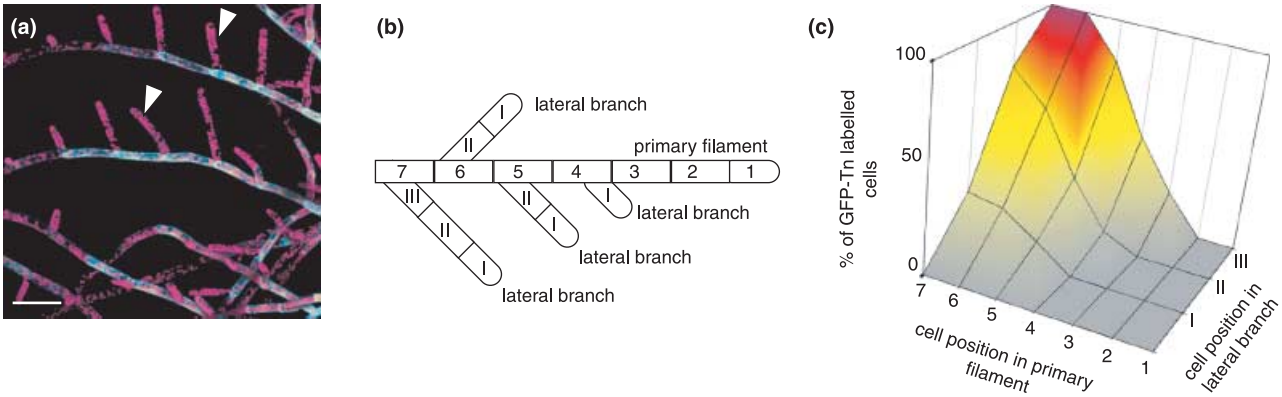

Fig. 2 Constitutive expression of green fluorescent protein (GFP)-talin in *Physcomitrella patens* protonemal tissue. (a) 35S-GT strain accumulating GFP signal in aged protonemal cells, but not in the emerging protonemal cells (arrowheads). (b) Schematic representation of the moss protonemal filament displaying positioning of cells in primary filament and lateral branches. (c) The distribution of labeled cells in the primary protonemal filaments and in the lateral outgrowing branches. Only cells at the sixth position and higher, as well as adjacent outgrowing branches are labeled. Bars, 100 μm.

Unlike the HGT lines, in 35S-GT lines GFP fluorescence could not be detected in all cell types; it was absent in protonema apical and subapical cells (Fig. 2a), in regenerating protoplasts young meristematic buds and young gametophores. To characterize further this effect of the 35S promoter, we determined the percentage of labeled cells relatively to their position along protonema filaments. The fraction of labeled cells was found to increase proportionally to the distance from the tip cells and reached a maximum at the sixth cell along the main filament and third cell along lateral branches (Fig. 2b,c). The same correlation was observed between cell position and actin labeling during spore germination and protoplast regeneration (data not shown). During filamentous growth, the position of the cell in the filament directly reflects its state of differentiation and, indeed, most cells that were labeled in 35S-GT lines were fully grown cells that had already completed their differentiation steps. With the weak 35S CaMV promoter, actively growing cells were not properly labeled; this promoter is therefore inappropriate for the study of the actin cytoskeleton dynamics in plants.

Tightly controlled amounts of GFP-talin are not detrimental to moss cells

High GFP-talin expression can affect the normal behavior of plant cells (Kost *et al.*, 1998; Kovar *et al.*, 2001; Timmers *et al.*, 2002; Ketelaar *et al.*, 2004; Sheahan *et al.*, 2004). We did not detect any alteration in growth or development of the 35S-GT plants, which completed their life cycle and were normally fertile. The same was true for the HGT strains grown at 25°C or submitted once to a 1-h HS at 37°C. This indicates that neither a weak constitutive, nor a single transient strong expression of GFP-talin can significantly affect the normal growth and development in *P. patens*. At the cellular level, we initiated our study on protoplasts, since their regeneration mimics spore germination. This also enabled us to study actin dynamics during the establishment of cell polarity and the restoration of polar outgrowth in a single cell. We regenerated wild-type (WT), 35S-GT and HGT protoplasts under standard conditions and in linearly polarized white light. Interestingly, we observed that the kinetic of cell division in heat-treated HGT protoplasts was delayed for approx. 24 h compared with untreated samples and other strains, albeit without affecting the cell survival or subsequent growth rate (data not shown). In linearly polarized light, the orientation of the electrical vector defines the orientation of cell division and of polar tip growth in moss protoplasts. We observed that the orientation of cell division and of polar outgrowth were identical in WT, 35S-GT and heat-treated HGT protoplasts derived colonies (data not shown).

Using iterative inductions, we tested the threshold of potential deleterious effects of excessive amounts of GFP-talin in moss tissues. This was achieved by comparing the moss development following either a single 1-h heat-treatment at

Fig. 1 Heat-induced expression of green fluorescent protein (GFP)-talin in *Physcomitrella patens* protonemal tissue of the HGT strain. (a) Immunoblot against GFP and actin using total protein extract isolated from the various heat-treated moss tissues. Total proteins were extracted 16 h after heat induction; n.i.; non-induced. (b) Confocal images showing heat-induced GFP-talin expression. Confocal images display fluorescence signal of GFP in green (left), auto fluorescence of chloroplasts in magenta (middle) and overlay (right). (c) Time-course of GFP-talin induction and turnover following optimal heat induction. The protonemal tissue was submitted to heat for 1 h at 37°C and observed at the indicated time following induction. Note that apical cells continue to grow during the period of 24 h (arrowhead). Bars, (b), 100 μm; (c), 50 μm.

37°C followed by a continuous week-long incubation at 25°C, or seven daily iterative heat treatments of 1 h separated by 23 h incubation at 25°C. The lengths of at least 15 apical protonema cells for each treatment at indicated time-point were measured and related to the produced amounts of GFP-talin (Fig. 3a,b). A single thermal induction of GFP-talin in the HGT strain caused no detectable alteration in cell length in apical protonema cells, as observed 1 day after induction (Figs 1c and 3a). At this point, the amount of GFP-talin was maximal; it then started to decline during the next 2 d to reach the initial basal level on day 4 (not shown). By contrast, single daily inductions over 1 wk resulted in the presence of a constant high amount of GFP-talin in the HGT strain (Fig. 3b), which resulted in a remarkable 50% inhibition of cell length at day 8. Repeatedly induced cells were found to be swollen with a disordered structure of the actin network (Fig. 3c–f). The 35S-GT strains used as control did not display any detectable morphological alterations after both types of thermal treatments (data not shown).

In summary, a single 1-h heat-induction is adequate to produce detectable transient amounts of GFP-talin that are able to clearly label F-actin in growing and differentiating cells, without any noticeable effect on cell growth, morphology and physiology. By contrast, the continuous expression of high amounts of GFP-talin in moss protonema tissue had damaging effects.

Cell polarization and restoration of apical growth in moss protoplasts is associated with the formation of F-actin apical arrays at the new growing site

Freshly isolated protoplasts from the HGT strain were embedded in agar and kept 24 h in darkness. They were regenerated in growth chambers and submitted to a single HS at the indicated times after isolation. The localization and organization of the F-actin network was observed by confocal microscopy. One-day-old protoplasts did not show any visible polarization; they displayed a cortical actin network formed by branched and randomly oriented thin actin cables occasionally connected to disperse small actin patches (Fig. 4a). A polarized pear-shaped aspect characterizes 2-d-old protoplasts. The strong polarization of the actin cytoskeleton is associated with the establishment at the growing tip of the cell of a large and diffused apical actin array interconnected with the cortical actin network (Fig. 4b). At day 3, cells have undergone their first division. The apical actin array is located at the growing pole of the new cell and a cortical actin network is visible in both cells (Fig. 4c). Diffused fluorescence was also detected in the cytoplasm of the new cell, suggesting active *de novo* F-actin synthesis. At day 5, the colony was formed by four to six cells (Fig. 4d). The cortical actin network is structurally very similar in all cells and the F-actin array is located at the tip of the apical cell. Newly formed F-actin arrays were also frequently observed in multicellular chloronemal colonies. Caps of F-actin were present at the tip zone of the apical cells and lateral structures were detected at the presumptive sites of new side branches. To confirm that these structures determine the site of the new side branches, we followed the fate of 20 of these actin arrays in 6-d-old protonema filaments. After GFP-talin induction, 16 of these structures gave rise to new cell outgrowth bearing the remaining GFP-talin (Fig. 5a–c).

The GFP-talin labeled actin cytoskeleton in protoplasts is a complex isotropic mesh-like structure. Cell polarization and restoration of apical growth in protonema filaments was associated with the formation of large F-actin arrays, which in turn determined new cell initials.

F-actin arrays and bundled actin network are the two main types of microfilament assemblies in protonemal cells

Optimal *in vivo* labeling of F-actin fluorescence made possible the detailed description of F-actin assemblies in all cells during the various growth and development phases of *P. patens*. Confocal imaging of apical chloronemal cells (Fig. 5d) revealed accumulation of F-actin at the very cell tip. In neighboring subapical cells, similar star-like structures that directly interconnected with actin cables were frequently observed. Following further development of the chloronemal filaments, the localized dense actin arrays were rarely observed in cells positioned at least six cells away from the apex (data not shown). In these differentiated chloronemal cells we observed randomly arranged actin bundles (Fig. 5e).

In the inner regions of the cell, the GFP-talin was detected in the nucleus (Fig. 5f). The same confocal projection revealed that these bundles were mainly located at the periphery of the cell. In a single confocal section, we could also observe a very fine meshwork of filaments surrounding each chloroplast (Fig. 5g). Similar to chloronemal cells, apical caulonemal cells contained a dense accumulation of fine cortical actin network localized in the apical zone (Fig. 5h). About one-third of the way down the cell axis, a dense network of longitudinally oriented actin strands was observed (Fig. 5i). In the subapical caulonemal cells, the numerous thick actin bundles were aligned in parallel and accumulated at the half of the cell oriented toward the apex, whereas they were less abundant at the corresponding cell end.

These results suggest that differences in the spatiotemporal organization of the F-actin structures are in close correlation with the physiological roles of the protonemal cells.

Organization of microfilament assemblies during gametophore development and leaf cell de-differentiation

We next addressed the organization of actin networks during the formation and the development of moss organs by caulinary growth. A GFP-decorated actin network was also

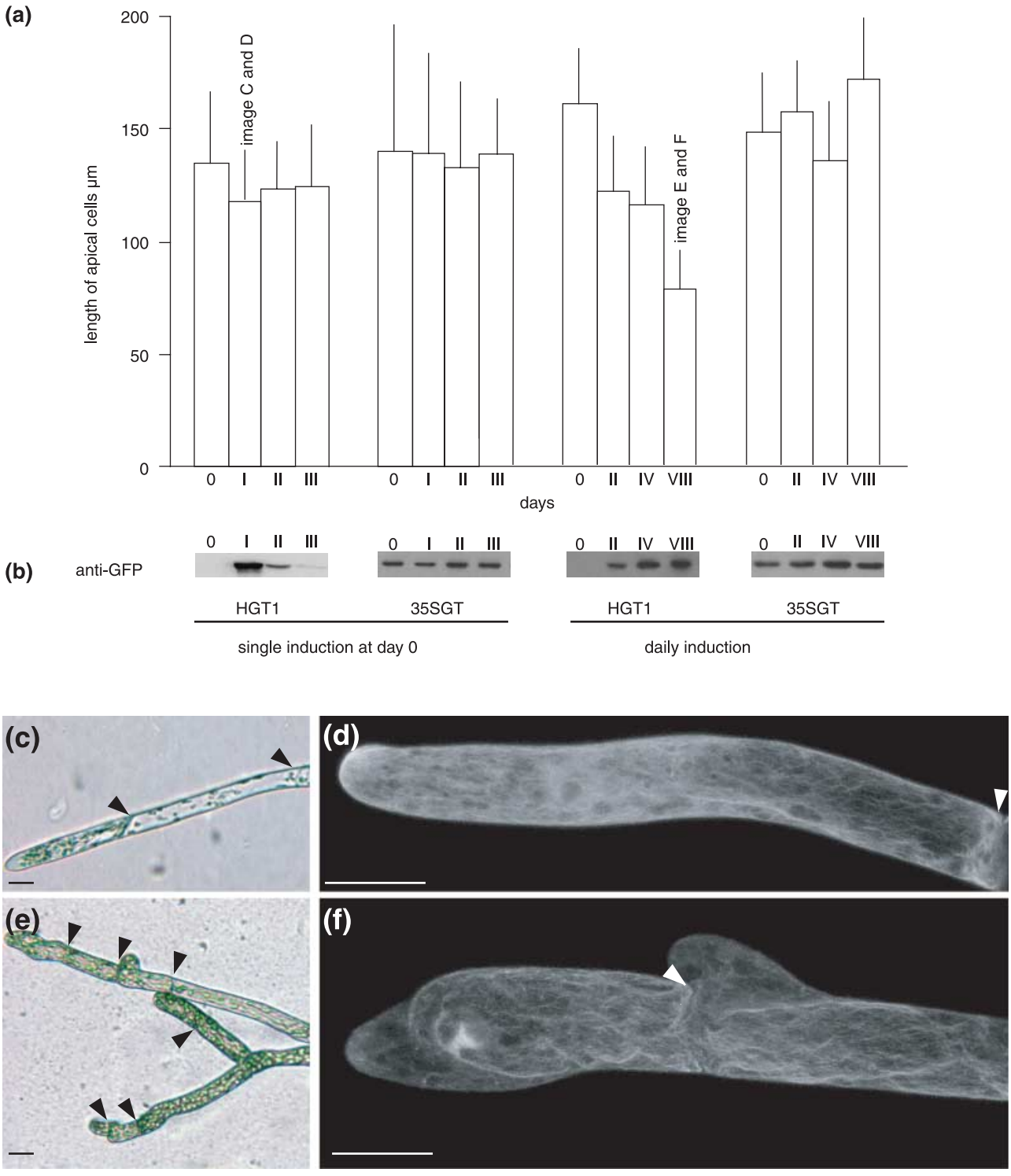

Fig. 3 Effect of green fluorescent protein (GFP)-talin accumulation after single induction or daily inductions in *Physcomitrella patens* protonemal cells. (a) Average length of apical protonemal cells in HGT and 35S-GT strains after a single thermal induction compared with iterative daily inductions. Single induction: 1-h heat shock at 37°C. Daily induction: 1-h heat shock at 37°C every day followed by 23 h at 25°C. Roman numerals are days after the first heat induction at which the cell measurements and corresponding immunoblots were performed. Data bars represent means and standard deviation of measurement of length of at least 20 fully grown apical cells. (b) Immunoblots showing the relative amounts of GFP-talin corresponding to each bar of (a). (c) Representative white-light and (d) confocal image of HGT1 protonemal filament taken 1 d after a single heat induction. (e) Representative white-light and (f) confocal images of HGT1 protonemal filament taken after eight iterative days of daily induction. Arrowheads indicate the transverse cell wall. GFP signal is white. Bars, 20 µm.

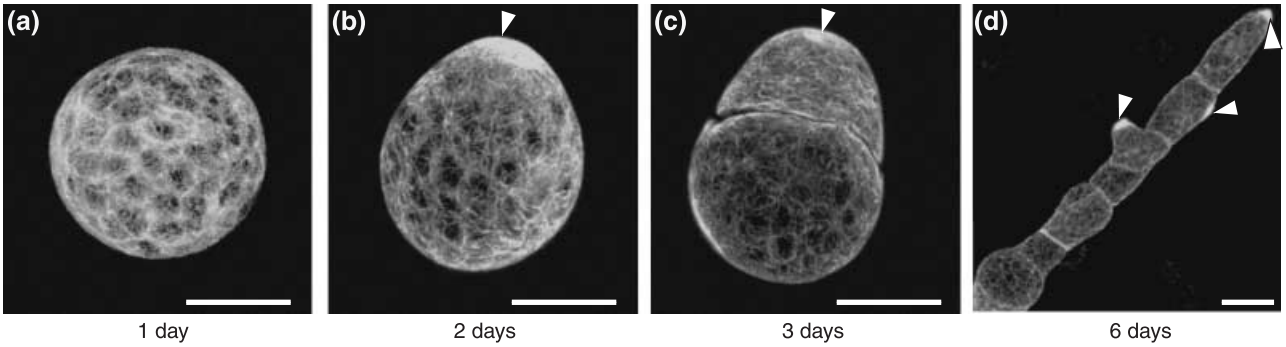

Fig. 4 Apical arrays of F-actin are associated with the new cell outgrowth. Freshly isolated *Physcomitrella patens* protoplasts were regenerated for 1, 2, 3 and 6 d, as indicated. Green fluorescent protein (GFP)-talin expression was induced by 1 h at 37°C and F-actin structures were observed 16 h after induction. (a) A 1-d-old spherical protoplast with uniform distribution of actin strands. (b) A 2-d-old asymmetric, pear-shaped protoplast with actin accumulation at the growing tip (arrowhead). (c) A 3-d-old mother cell and apical daughter cell obtained from an asymmetric cell division, which maintained F-actin accumulation in the growing tip. (d) A 6-d-old protonemal filament containing F-actin that accumulates at the tip of the apical chloronemal cells. Prominent F-actin accumulation is also visible in subsequent subapical cells determining outgrowth of lateral cell (arrowheads).Bars, 20 μm; step size (a–c),160 nm.

observed in tissue older than 2 wk, grown on solid minimal medium. In the emerging buds, the youngest meristematic cells displayed a dense network of apparently nonoriented microfilaments, with two or three prominent actin arrays per cell (Fig. 6a). Cells forming the base of the gametophore, as well as those in surrounding meristems, contained a distinct network of actin cables. Apical rhizoids emerging from the base of the gametophores possessed a network of actin cables that converged to an F-actin array that was slightly displaced from the apex. (Fig. 6b). Following further development, the cells of juvenile leaves of gametophores (Fig. 6c) were characterized by the presence of cortical F-actin patches, which could clearly be distinguished from cytoplasmic F-actin bundles also present in these cells. To our knowledge, this is the first time that such F-actin patches have been described in developing plant leaves. These assemblies were occasionally observed in the basal part of adult leaves from 1-month-old gametophores, but a bundled actin network was the dominant form of the actin cytoskeleton in these cells (Fig. 6d). These data suggest that the transition from unidirectional development to a caulinary growth is associated with the formation of complex F-actin assemblies, depending on the specific developmental stage of each cell. The homogeneous presence of bundled actin network in every leaf cell appeared to be typical for the terminal stage of cell differentiation.

The fate of the large actin bundles in mature leaf cells was investigated during artificial dedifferentiation. To induce dedifferentiation, 20 adult leaves from 2-wk-old gametophores were cut and placed on solid minimal medium supplemented with nitrogen and carbon source (see the Materials and Methods section). In freshly cut leaf, GFP-talin synthesis was induced by heat treatment and the fate of the aforementioned network of actin bundles was monitored in each cell. After 2 d, some of these cells started to divide and showed a diffuse mesh of actin fibers, different from the mature nondividing cells (Fig. 6e). Dividing cells contained half-sized chloroplasts, compared with undivided neighboring cells. In order to monitor the destiny of these cells, we followed in time the outcome of 10 such regions on three different leaves. We followed the outcome of 10 cells induced to divide by the dedifferentiation regime on three different leaves. On the third day, protonemal filaments containing two cells were seen to protrude from four of the previously dedifferentiated leaf cells; on day six protonema formation was seen on all cells. In the

Fig. 5 Labeled F-actin arrays are present during development and differentiation of protonemal cells of *Physcomitrella patens*. Green fluorescent protein (GFP)-talin expression is induced in 6-d-old protonemal cells and GFP signals were allocated 1 d after heat induction in green (a) and on the same tissue, 2 d following the thermal induction in magenta (b). The arrows indicate bright F-actin arrays and arrowheads denote emerging cell outgrowth. (c) Overlay image shows newly formed cells where previously F-actin array were observed. (d–i) Detailed confocal images displaying actin organization in moss protonemal cells. Left panels, fluorescence signal of GFP in white; right panels, overlay representing auto fluorescence of chloroplasts in magenta and GFP. (d) In apical chloronemal cells, F-actin forms a radial cap structure at the very tip of the cell (arrowhead). A similar array is visible in the adjacent cell. (e) Chloronemal subapical cell with a defined network of actin bundles. (f) The same cells as from (e) showing internal confocal projection of 30 optical sections from the medial region representing the nucleus (arrows) and cytoplasmic strands. (g) Single confocal section representing the boxed region from (e), displaying a subcortical network of actin bundles surrounding the chloroplasts. (h) A juvenile apical caulonemal cell containing an apical cap structure with a dense network of actin cables. (i) A differentiated subapical caulonemal cell with apicobasal distribution of actin bundles. Bars, (a–f,h,i) 20 μm, (g) 5 μm. Step size: (a–c) 630 nm, (d–f,h,f) 160 nm.

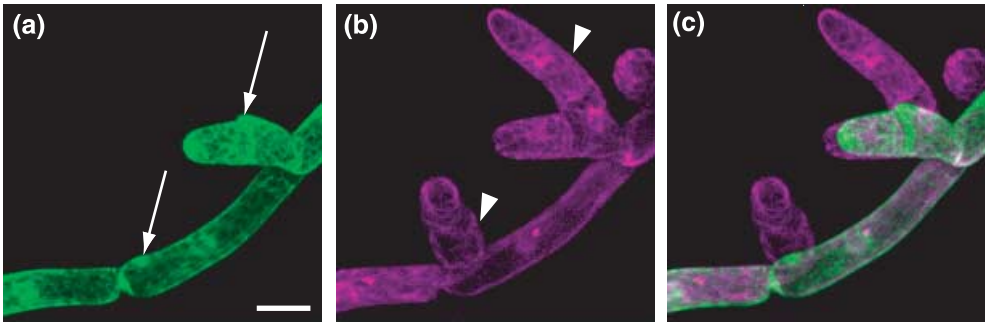
(a)
(b)
(c)
1 day after induction
2 days after induction
merged

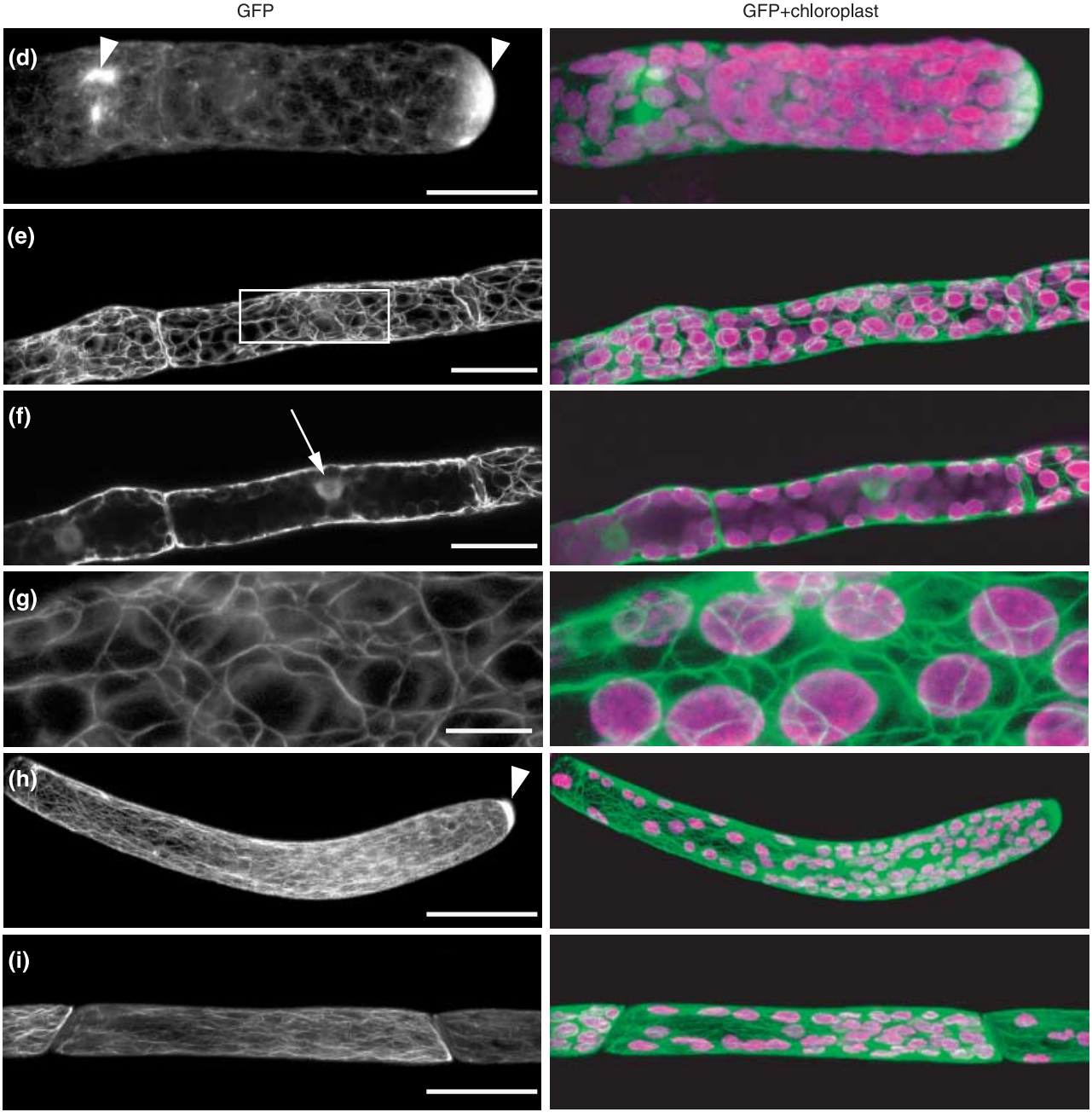
GFP
GFP+chloroplast
(d)
(e)
(f)
(g)
(h)
(i)

new outgrowing cells, the actin network included apical actin arrays and diffuse F-actin strands, which were indistinguishable from those detected in apical chloronemal cells (Fig. 6f). Here, we demonstrated that the processes of dedifferentiation and rapid growth involve a radical change in the spatial organization of the actin microfilaments network – a rearrangement that precedes outgrowth of new cells.

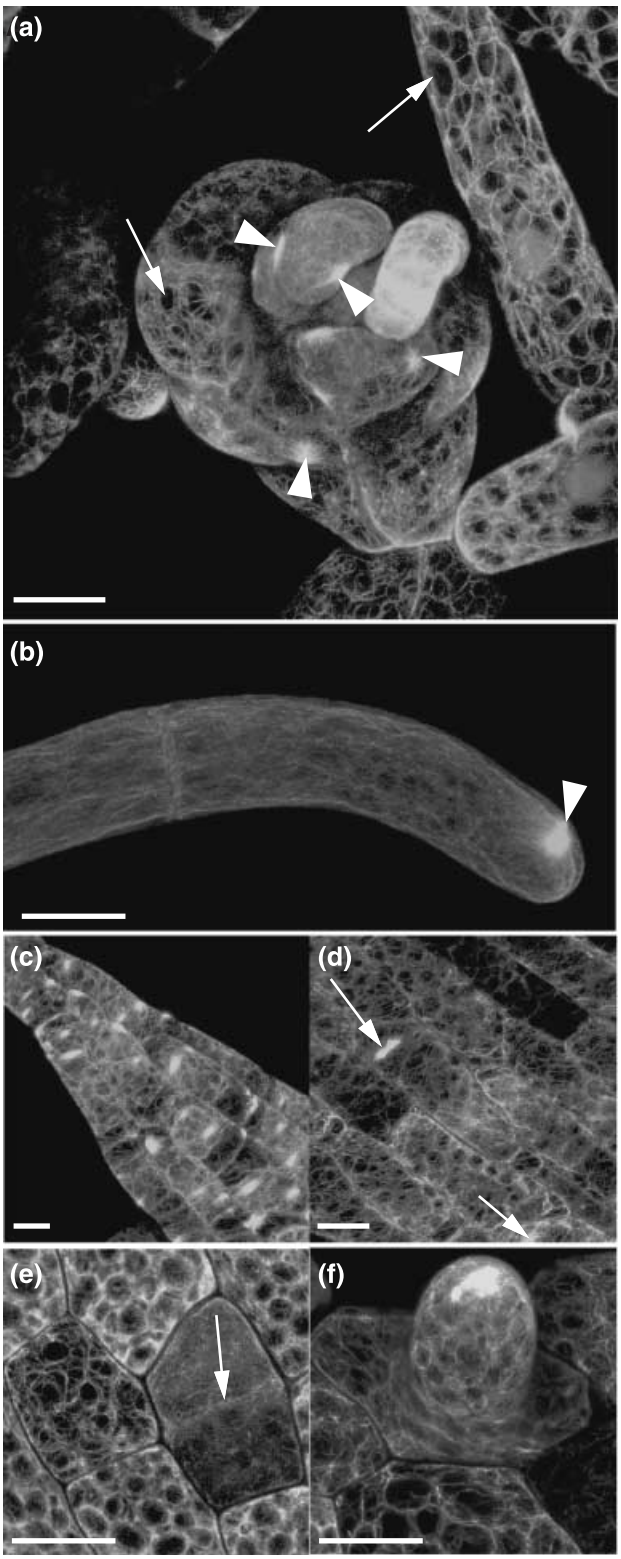

Cytoskeleton inhibitors and mutations affecting the organization of F-actin arrays result in an altered morphology of chloronemal cells

Specific chemical inhibitors are important tools to study the function of cytoskeleton elements. Actin depolymerizing drugs such as cytochalasins, drastically reduce cell expansion (Geitmann & Emons, 2000). Treatments with microtubule drugs, such as oryzalin or taxol cause swelling of cells in the leaf epidermis, hypocotyl and root (Baskin *et al.*, 1994). Mutations affecting essential microfilament components like those in the ARP2/3 complex are also informative in this respect.

In order to confirm that GFP-talin labeled structures are actin microfilaments, we grew protonemal tissues for 4 d on medium containing the F-actin disrupting drugs cytochalasin B and latrunculin B or the microtubule-disrupting drug oryzalin, at final concentrations of 10 μM, 5 μM and 3 μM, respectively. GFP-talin was then induced and 16 h later cytoskeleton and morphological alterations were imaged. Unlike untreated chloronemal cells (Fig. 7a,b), the actin cable network was seriously distorted in emerging subapical chloronemal cells continuously treated by cytochalasin B, and F-actin caps were deformed (Fig. 7c,d). Further incubation with cytochalasin B inhibited growth of newly formed cells, which were approximately half as long as untreated cells. Treatment with latrunculin B created strong morphological alterations, changing the cylindrical shape of the protonemal cells to ball-like. Confocal imaging of these cells displayed strongly reduced apical actin arrays and the disorganized network formed short actin bundles (Fig. 7e,f). The oryzalin induced bulging in growing protonemata and the characteristic F-actin cap appeared at the bulging end, whereas a network of

Fig. 6 Labeled F-actin arrays during development of the gametophore of *Physcomitrella patens*. (a) Proliferating bud showing the complex organization of the actin network. The star-like actin arrays (arrowheads) as well as the areas of dense and diffuse actin are found in the youngest meristematic cells. Regular 'gaps' in the actin network indicate the position of chloroplasts (arrows). (b) Tip cell of rhizoid filament containing apical actin array (arrowhead). (c) Part of the leaf of juvenile gametophore, in which every cell contains at least one star-like actin array. (d) Detailed image of part of the leaf of an adult gametophore displaying the structural organization of actin bundles in leaf cells; only a few star-like actin arrays are visible (arrows). (e,f) Representative images showing labeled actin network in cells from a leaf 2 d and 4 d after excision, respectively. (e) After 2 d, there is diffuse fluorescence in newly divided cells (arrow) compared with the neighboring cells where the cable network is still visible. (f) After 4 d, differentiating chloronemal cell grows with prominent apical F-actin array. Bars, (a–c,e–j), 20 μm, (d) 5 μm. Step size, 160 nm.

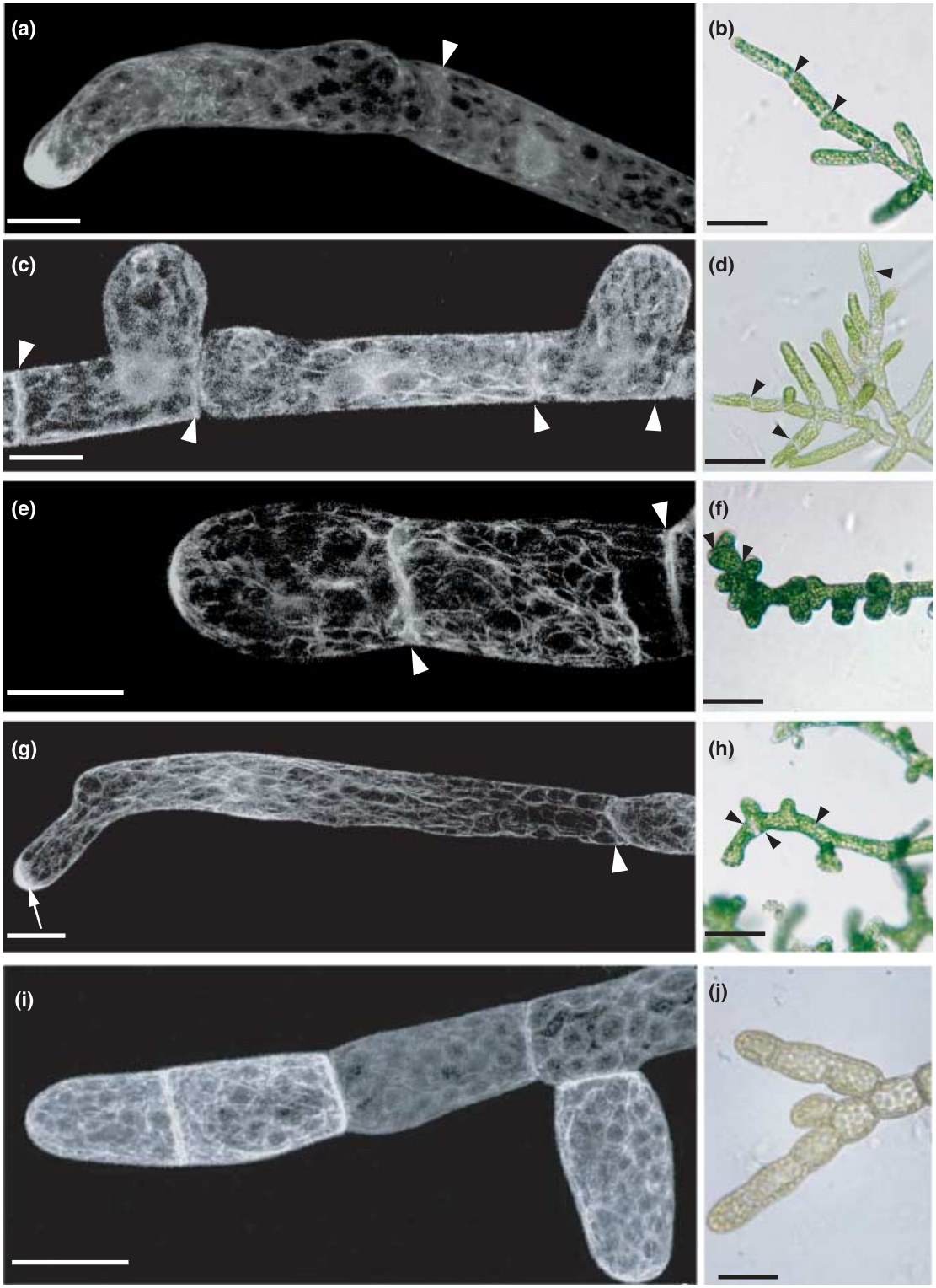

Fig. 7 Effect of cytoskeleton disrupting drugs and mutation on microfilament network and cell growth of *Physcomitrella patens*. Representative confocal projections (a,c,e,g,i) and transmission microscope images (b,d,f,h,j) are shown. (a,b) HGT1 untreated. (c,d) Cytochalasin B causes loss of actin caps in outgrowing cells and destroys cable network. Note that that treated cells are shorter than untreated ones. Arrowheads indicate cell wall between adjacent cells. (e,f) Latrunculin B destabilizes formation of apical actin arrays, disorganizes the network of actin filaments and causes dwarf growth. (g,h) Oryzalin provokes the appearance of the F-actin cap at the bulging site, reorienting the actin cables. *arp3*-ko insertional mutant line obtained by disruption of the ARP3 locus through homologous recombination (i,j); one can observe the absence of the WT normal apical star-like structure. Bars, confocal 20 μm, white light 100 μm.

bundled actin cables was reoriented toward the tip (Fig. 7g,h). This demonstrates that cytochalasin B and latrunculin B have a specific deleterious effect on F-actin structures, such as bundles and apical arrays, resulting in shortened cells. Oryzalin induced the displacement of F-actin arrays, leading to disoriented cell polar outgrowth.

Knockout mutations of the *arp3* gene (coding for one component of the ARP2/3 complex) induce a strong phenotypic response. In the protonemata, apical cap structures (actin patches present in normal wild-type plants) were not observed in the mutant; subcortical actin filaments are shorter, thicker and appear more diffuse, with no preferential orientation (Fig. 7i). The lack of properly organized actin arrays related to the *arp3* mutation result in altered and abnormal cell growth (Fig. 7j). The absence of these localized F-actin accumulations in the mutant, despite a strong GFP-talin expression, may indicate that their formation is Arp2/3 complex-dependent.

Discussion

Controlled expression of GFP-talin circumvents its damaging effect on plant cell growth

We used transgenic lines of the moss *P. patens* capable of conditionally expressing detectable amounts of GFP fused to the F-actin binding domain of mouse talin – GFP-talin (Kost *et al.*, 1998) – under the highly controllable heat-inducible promoter *Gmhsp17.3B* promoter. We achieved a transient labeling of the actin network without apparent negative effects of the GFP-talin protein on cellular morphology and development. The F-actin features in all the cells at all developmental stages of the moss gametophyte were efficiently labeled: isolated protoplasts, regenerating protoplasts, apical, subapical protonemal cells, buds and leafy shoots of gametophores. Our results corroborate previous observations in which transient GFP-talin expression allowed the visualization of the fine cortical actin network, as well as of thick actin bundles in several model plant cell types (Fu *et al.*, 2001; Jones *et al.*, 2002).

It has been shown in a transgenic moss strain containing the *uidA* gene driven by *Gmhsp17.3B* promoter that GUS activity is very low while the moss is kept at 25°C and may be induced up to three orders of magnitude following a mild heat-treatment (Saidi *et al.*, 2005). Maximal expression levels in the heat-inducible GUS strain has been at least 300-, 20- and 10-fold higher than levels measured in transgenic lines carrying the *uidA* gene driven by the CaMV-35S, the rice actin (*act-1*) and the maize ubiquitin (*ubi-1*) promoters, respectively. We produced transgenic moss lines constitutively expressing GFP-talin from the CaMV-35S promoter, in which GFP-talin accumulated in detectable amounts only in aged cells indicating that the weak constitutive activity of 35S promoter was not sufficient to overcome the level of natural fluorescence detection in juvenile cells. However, our attempts to generate strains expressing GFP-talin from the strong constitutive rice *act-1* promoter have not been successful. Our results for the toxicity of constitutively expressed GFP-talin in the HGT lines confirmed that the *act-1* promoter must have generated excessive high levels of GFP-talin that were detrimental to the early stages of protoplast regeneration. Similarly, multiple induction of GFP-talin in the HGT lines blocked regeneration in protoplasts derived from the HGT strain (data not shown). The deleterious effects caused by excess of GFP-talin confirms the inhibitory effects of constitutively expressed GFP-talin on tobacco pollen tubes (Kost *et al.*, 1998) and on *Arabidopsis* root hair (Ketelaar *et al.*, 2004). The results of Ketelaar and colleagues have been interpreted in terms of GFP-talin being a poor choice as a reporter of actin microfilaments. Our data indicate that the stable presence of high amounts of GFP-talin may indeed cause morphological alterations in moss cells. We surmise that protoplasts may be more susceptible to GFP-talin expression than protonemal cells, possibly because GFP-talin may not have same affinity for differentially expressed F-actin at particular stage of moss development.

Subcellular actin arrays faithfully reflect the differentiation status of the cell

During moss protoplast regeneration, the organization of a polar axis precedes the polar outgrowth (Cove, 1992). Our results on F-actin localization during the cell polarization demonstrate that F-actin accumulations are associated with sites of outgrowth at the filamentous unicellular stage of moss development (Fig. 4). This strengthens earlier studies on *Fucus* and *Pelvetia* embryos, using rhodamine–phalloidin staining, that showed F-actin accumulation at the prospective site of rhizoid poles (Kropf *et al.*, 1989; Alessa & Kropf, 1999). Similar actin arrays visualized by rhodamine–phalloidin were described in protonemal cell of *Funaria hygrometrica* during side-branch initiation in protonemal cells (Quader & Schnepf, 1989). We showed clearly that star-like microfilament arrays determine the position of cell outgrowth of protonemal cells and rhizoids (Figs 4–6). The bundled actin networks have been imaged in differentiated subapical chloronemal and caulonemal cells at high resolution. Morphological differences between chloronemal and caulonemal cells (Schumaker & Dietrich, 1997) were shown at the level of the actin cytoskeleton. The photosynthetic subapical chloronemal cells have a bundled actin network that may serve as support for chloroplast movement (Sato *et al.*, 2001), whereas organization of longitudinal actin strands implies their role in polar transport of fast-growing caulonemal cells. *Physcomitrella patens* undergoes a transition from a filamentous growth phase to a caulinary growth phase, during which, apico-basal growth is replaced by diffuse growth, involving multiple lateral interactions between cells in buds and leaves. Initial studies of visualization of moss actin cytoskeleton using rhodamine–phalloidin focused on protonemal tissue and did

not provide relevant information about organization of the actin cytoskeleton in gametophores (Doonan *et al.*, 1988; Quader & Schnepf, 1989; Meske & Hartmann, 1995; Walker & Sack, 1995). In this study, we were able to follow in time and space the fate of the actin cytoskeleton during this major growth phase transition. For the first time, significant rearrangements of F-actin were found, from fine filaments in meristematic cells of buds and young leafy gametophytes to spider web-like cytoskeleton actin organization in differentiated leaf cells of adult gametophores (Fig. 6). Whereas networks of bundled actin cables have been observed in epidermal cells of *Arabidopsis* leaves (Kost *et al.*, 1998), we present strong support for the existence of cortical F-actin array in young leaf cells of *P. patens* that have never been imaged previously. In conclusion, our data validate the fact that F-actin arrays reflect cellular differentiation status.

Proper F-actin is required for the expansion of moss protonemal cells

Several reports have proposed that F-actin mediates the delivery of Golgi-derived vesicles to the plasma membrane of diffusely growing cells and in tip-growing cells (Baskin & Bivens, 1995; Miller *et al.*, 1999; Dong *et al.*, 2001). Inhibitory studies performed on root hairs, pollen tubes and trichomes, emphasize the central role of the actin cytoskeleton in cellular expansion (Gibbon *et al.*, 1999; Mathur *et al.*, 1999; Miller *et al.*, 1999; Hepler *et al.*, 2001; Vidali *et al.*, 2001), whereas microtubules would determine the sites of plant cellular growth (Mathur & Hulskamp, 2002). We found here that treatment of protonemal cells with actin depolymerizing drugs cytochalasin B and latrunculin B eliminates the apical F-actin arrays and disorganizes actin network, which in turn affects cell growth. Conversely, the microtubule inhibitor oryzalin caused sinusoid growth leaving the actin-filled dome still visible (Fig. 7). The effects of selective depletion of F-actin arrays indicate that actin cytoskeleton is involved in vesicle accumulation at the growth site of protonemal cells. It has recently been demonstrated that latrunculin B, a potent inhibitor of actin polymerization (Harries *et al.*, 2005), phenocopied the alteration of protoplast regeneration that was caused by the RNAi approach reducing the amount of ArpC1 subunit of the Arp2/3 complex, the principal actin nucleating protein assembly. Perroud & Quatrano (2006), showed that, in *P. patens*, a deletion of ARPC4, another member of the Arp2/3 complex, resulted in abnormal extension growth; caulonemal cells were nevertheless formed (Perroud & Quatrano, 2006). It should be verified whether the null mutant Δ*arpc1* phenotype would be similar to the phenotype obtained by RNAi silencing; ARPC1RNAi could well affect the expression of other genes involved in moss developmental pathways.

The use of moss transgenic plants that conditionally express GFP-talin would allow the visualization of the interplay between different cytoskeleton elements *in planta*. Initial observations on moss transgenic mutant containing a disrupted *arp3* gene show that F-actin foci are not present, whereas morphogenesis and differentiation of tip-growing cells is drastically altered (Fig. 7i,j). Further studies using mutants plants affected in proteins involved in the maintenance of the cytoskeleton are feasible in *P. patens* using allele replacement or gene disruption; proper visualization F-actin organization during cell morphogenesis and plant development can also be achieved.

Acknowledgements

We thank Dr Nam-Hai Chua for kindly providing us with the pYSC14 plasmid. This work was supported in part by Swiss National Science Foundation Grants #31-51853.97 and #31-65211.01.

References

Alessa L, Kropf DL. 1999. F-actin marks the rhizoid pole in living *Pelvetia compressa* zygotes. *Development* **126**: 201–209.

Ashton NW, Cove DJ. 1977. Isolation and preliminary characterization of auxotrophic and analog resistant mutants of moss, *Physcomitrella patens*. *Molecular and General Genetics* **154**: 87–95.

Baskin TI, Bivens NJ. 1995. Stimulation of radial expansion in *Arabidopsis* roots by inhibitors of actomyosin and vesicle secretion but not by various inhibitors of metabolism. *Planta* **197**: 514–521.

Baskin TI, Wilson JE, Cork A, Williamson RE. 1994. Morphology and microtubule organization in *Arabidopsis* roots exposed to oryzalin or taxol. *Plant and Cell Physiology* **35**: 935–942.

Cove D. 1992. Regulation of development in the moss, *Physcomitrella patens*. In: Russo VEA, Brody S, Cove D, Ottolenghi S, eds. *Development: the molecular genetic approach*. Berlin, Germany: Springer-Verlag, 179–193.

Dong CH, Xia GX, Hong Y, Ramachandran S, Kost B, Chua NH. 2001. ADF proteins are involved in the control of flowering and regulate F-actin organization, cell expansion, and organ growth in *Arabidopsis*. *Plant Cell* **13**: 1333–1346.

Doonan JH, Cove DJ, Lloyd CW. 1988. Microtubules and microfilaments in tip growth – evidence that microtubules impose polarity on protonemal growth in *Physcomitrella patens*. *Journal of Cell Science* **89**: 533–540.

El-Assall SE, Le J, Basu D, Mallery EL, Szymanski DB. 2004. DISTORTED2 encodes an ARPC2 subunit of the putative *Arabidopsis* ARP2/3 complex. *Plant Journal* **38**: 526–538.

Fu Y, Wu G, Yang ZB. 2001. Rop GTPase-dependent dynamics of tip-localized F-actin controls tip growth in pollen tubes. *Journal of Cell Biology* **152**: 1019–1032.

Geitmann A, Emons AMC. 2000. The cytoskeleton in plant and fungal cell tip growth. *Journal of Microscopy – Oxford* **198**: 218–245.

Gibbon BC, Kovar DR, Staiger CJ. 1999. Latrunculin B has different effects on pollen germination and tube growth. *Plant Cell* **11**: 2349–2363.

Harries PA, Pan AH, Quatrano RS. 2005. Actin-related protein2/3 complex component ARPC1 is required for proper cell morphogenesis and polarized cell growth in *Physcomitrella patens*. *Plant Cell* **17**: 2327–2339.

Hepler PK, Vidali L, Cheung AY. 2001. Polarized cell growth in higher plants. *Annual Review of Cell and Developmental Biology* **17**: 159–187.

Jones MA, Shen JJ, Fu Y, Li H, Yang Z, Grierson CS. 2002. The *Arabidopsis* Rop2 GTPase is a positive regulator of both root hair initiation and tip growth. *Plant Cell* **14**: 763–776.

Ketelaar T, Anthony RG, Hussey PJ. 2004. Green fluorescent protein-talin causes defects in actin organization and cell expansion in *Arabidopsis* and

inhibits actin depolymerizing factor's actin depolymerizing activity *in vitro*. *Plant Physiology* **136**: 3990–3998.

Kost B, Spielhofer P, Chua N-H. 1998. A GFP-mouse talin fusion protein labels plant actin filaments *in vivo* and visualises the actin cytoskeleton in growing pollen tubes. *The Plant Journal* **16**: 393–401.

Kost B, Bao YQ, Chua NH. 2002. Cytoskeleton and plant organogenesis. *Philosophical Transactions of the Royal Society of London Series B, Biological Sciences* **357**: 777–789.

Kovar DR, Gibbon BC, McCurdy DW, Staiger CJ. 2001. Fluorescently-labeled fimbrin decorates a dynamic actin filament network in live plant cells. *Planta* **213**: 390–395.

Kropf DL, Berge SK, Quatrano RS. 1989. Actin localization during *Fucus* embryogenesis. *Plant Cell* **1**: 191–200.

Kwok EY, Hanson MR. 2004. *In vivo* analysis of interactions between GFP-labeled microfilaments and plastid stromules. *BMC Plant Biology* **4**: 2.

Lowry OH, Rosebrough NJ, Farr AL, Randall RJ. 1951. Protein measurement with the folin phenol reagent. *Journal of Biological Chemistry* **193**: 265–275.

Mathur J, Hulskamp M. 2002. Microtubules and microfilaments in cell morphogenesis in higher plants. *Current Biology* **12**: R669–R676.

Mathur J, Spielhofer P, Kost B, Chua NH. 1999. The actin cytoskeleton is required to elaborate and maintain spatial patterning during trichome cell morphogenesis in *Arabidopsis thaliana*. *Development* **126**: 5559–5568.

McElroy D, Blowers AD, Jenes B, Wu R. 1991. Construction of expression vectors based on the rice actin-1 (Act1) 5′ region for use in monocot transformation. *Molecular and General Genetics* **231**: 150–160.

Meske V, Hartmann E. 1995. Reorganization of microfilaments in protonemal tip cells of the moss *Ceratodon purpureus* during the phototropic response. *Protoplasma* **188**: 59–69.

Miller DD, de Ruijter NCA, Bisseling T, Emons AMC. 1999. The role of actin in root hair morphogenesis: studies with lipochito-oligosaccharide as a growth stimulator and cytochalasin as an actin perturbing drug. *Plant Journal* **17**: 141–154.

Perroud PF, Quatrano RS. 2006. The role of ARPC4 in tip growth and alignment of the polar axis in filaments of *Physcomitrella patens*. *Cell Motility and the Cytoskeleton* **63**: 162–171.

Quader H, Schnepf E. 1989. Actin filament array during side branch initiation in protonema cells of the moss *Funaria hygrometric*a – an actin organizing center at the plasma-membrane. *Protoplasma* **151**: 167–170.

Saidi Y, Finka A, Chakhparonian M, Zryd J-P, Schaefer D, Goloubinoff P. 2005. Controlled expression of recombinant proteins in *Physcomitrella patens* by a conditional heat-shock promoter: a tool for plant research and biotechnology. *Plant Molecular Biology* **59**: 697–671.

Sato Y, Wada M, Kadota A. 2001. Choice of tracks, microtubules and/or actin filaments for chloroplast photo-movement is differentially controlled by phytochrome and a blue light receptor. *Journal of Cell Science* **114**: 269–279.

Schaefer DG. 2001. Gene targeting in *Physcomitrella patens*. *Current Opinion in Plant Biology* **4**: 143–150.

Schaefer DG, Zryd JP. 1997. Efficient gene targeting in the moss *Physcomitrella patens*. *Plant Journal* **11**: 1195–1206.

Schaefer DG, Zryd JP. 2001. The moss *Physcomitrella patens*, now and then. *Plant Physiology* **127**: 1430–1438.

Schnepf E, Deichgraber G, Bopp M. 1986. Growth, cell-wall formation and differentiation in the protonema of the moss, *Funaria hygrometrica* – effects of plasmolysis on the developmental program and its expression. *Protoplasma* **133**: 50–65.

Schumaker KS, Dietrich MA. 1997. Programmed changes in form during moss development. *Plant Cell* **9**: 1099–1107.

Sheahan MB, Staiger CJ, Rose RJ, McCurdy DW. 2004. A green fluorescent protein fusion to actin-binding domain 2 of *Arabidopsis* fimbrin highlights new features of a dynamic actin cytoskeleton in live plant cells. *Plant Physiology* **136**: 3968–3978.

Smith LG. 2003. Cytoskeletal control of plant cell shape: getting the fine points. *Current Opinion in Plant Biology* **6**: 63–73.

Takemoto D, Jones DA, Hardham AR. 2003. GFP-tagging of cell components reveals the dynamics of subcellular re-organization in response to infection of *Arabidopsis* by oomycete pathogens. *Plant Journal* **33**: 775–792.

Timmers ACJ, Niebel A, Balague C, Dagkesaruanskaya A. 2002. Differential localisation of GFP fusions to cytoskeleton-binding proteins in animal, plant, and yeast cells. *Protoplasma* **220**: 69–78.

Vidali L, McKenna ST, Hepler PK. 2001. Actin polymerization is essential for pollen tube growth. *Molecular Biology of the Cell* **12**: 2534–2545.

Walker LM, Sack FD. 1995. Microfilament distribution in protonemata of the moss *Ceratodon*. *Protoplasma* **189**: 229–237.

Wasteneys GO, Galway ME. 2003. Remodeling the cytoskeleton for growth and form: an overview with some new views. *Annual Review Plant Biology* **54**: 691–722.